

# Relationship between structure and point of zero surface charge for molybdenum and tungsten oxides supported on alumina

S.D. Kohler, J.G. Ekerdt \*

*Department of Chemical Engineering, The University of Texas at Austin, Austin, TX 78712, USA*

D.S. Kim and I.E. Wachs

*Zettlemoyer Center for Surface Studies, Department of Chemical Engineering, Lehigh University, Bethlehem, PA 18015, USA*

Received 21 May 1992; accepted 12 August 1992

Laser Raman spectroscopy was used to characterize alumina-supported molybdenum and tungsten oxides at loadings ranging from 0.5 to 15 wt% Mo and 0.5 to 30 wt% W. The structure of calcined  $\text{Mo}^{6+}/\text{Al}_2\text{O}_3$  and  $\text{W}^{6+}/\text{Al}_2\text{O}_3$  was governed by the point of zero surface charge of each system, with the point of zero surface charge being dependent on metal loading. The structures formed by the molybdenum and tungsten overlayers at the sample point of zero surface charge were found to be analogous to the structures formed by molybdenum and tungsten oxyanions in aqueous solution at a solution pH equal to the sample point of zero surface charge.

**Keywords:** Molybdenum oxide; tungsten oxide; Raman spectroscopy; alumina; point of zero surface charge

## 1. Introduction

Laser Raman spectroscopy (LRS) has been used extensively to determine the structures of the molybdenum [1–14] and tungsten [15–19] oxide overlayers that form when one metal oxide component is deposited upon a different metal oxide support such as  $\text{Al}_2\text{O}_3$ ,  $\text{SiO}_2$ , and  $\text{TiO}_2$ . Although there have been differences in opinion involving the structure of the oxide overlayers in the past, it has been recently demonstrated that the structure of the overlayers under ambient conditions is analogous to the structure of the metal oxyanion in

\* To whom correspondence should be addressed.

aqueous solution [13,14,20]. Under ambient conditions, the oxide surfaces readily adsorb significant amounts of water from the environment. The hydrated molecular structures formed in the overlayers are reasoned to depend upon the pH at which the surface has zero net surface charge (point of zero surface charge (PZC)).

Williams et al. [14] have examined  $\text{MoO}_3/\text{Al}_2\text{O}_3$  samples prepared from  $\text{Mo}_2(\eta^3\text{-C}_3\text{H}_5)_4$ ,  $\text{H}_2(\text{MoO}_3\text{C}_2\text{O}_4) \cdot 2\text{H}_2\text{O}$ , and  $(\text{NH}_4)_6\text{Mo}_7\text{O}_{24} \cdot 4\text{H}_2\text{O}$  at loadings ranging from 0.67 to 13.3 wt% Mo with LRS. At low molybdenum loadings (< 1% Mo), a tetrahedrally-coordinated surface molybdate species predominated that was characterized by the  $\nu_s(\text{Mo-O})$  mode at  $930\text{--}916\text{ cm}^{-1}$  and the  $\delta(\text{Mo-O})$  mode at  $320\text{ cm}^{-1}$ . At high molybdenum loadings (> 6.7% Mo), the surface overlayer consisted mainly of octahedrally-coordinated heptamolybdate and octamolybdate species. The heptamolybdate and octamolybdate species were characterized by Raman bands at  $975\text{--}950\text{ cm}^{-1}$ ,  $360\text{--}350\text{ cm}^{-1}$ , and  $220\text{ cm}^{-1}$ , which are associated with the  $\nu(\text{Mo-O})$ ,  $\delta(\text{Mo-O})$ , and  $\text{Mo-O-Mo}$  deformation, respectively [3,4,10,13,14]. The hydrated structure of the calcined  $\text{Mo}^{6+}$  oxide overlayer on alumina was reasoned to depend only upon the PZC of the molybdena/alumina system [14]. The surface molybdenum oxide structure was found to be independent of preparation pH and precursor. Similar conclusions were drawn for the supported vanadate system [20]; the hydrated two-dimensional molecular structures of the vanadate overlayer were predicted at high and low coverages of vanadium by using reported PZC values. The predicted structures correlated very well with vanadate structures observed with LRS. Reported PZC values were also used to predict the structure of various metal oxide overlayers ( $\text{CrO}_3$ ,  $\text{MoO}_3$ ,  $\text{Re}_2\text{O}_7$ ,  $\text{V}_2\text{O}_5$ , and  $\text{WO}_3$ ) on different oxide supports ( $\text{Al}_2\text{O}_3$ ,  $\text{MgO}$ ,  $\text{SiO}_2$ ,  $\text{TiO}_2$ ,  $\text{ZrO}_2$ ) under ambient conditions [20].

The tetrahedral  $\text{WO}_4^{2-}$  is observed in aqueous solution above pH of  $\approx 7.8$  and 1 M in total tungsten [21,22]. At pH values near 7.8 and 1 M in total tungsten, the octahedral  $\text{W}_{12}\text{O}_{42}^{12-}$  polyanion forms and it persists until a pH of 5.7 [21]. Below a pH of 5.7, additional octahedrally-coordinated  $\text{W}_{12}$  polyanions form, such as  $\text{W}_{12}\text{O}_{39}^{6-}$ . The tetrahedral  $\text{WO}_4^{2-}$  anion and octahedral  $\text{W}_{12}\text{O}_{42}^{12-}$  polyanion will coexist in a solution at a pH near 7.8. Similarly, a solution at a pH near 5.7 will contain both octahedral  $\text{W}_{12}$  polyanions.

The PZC has been primarily used in catalysis to describe the adsorption behavior of solids. An electrostatic model [23,27], in which adsorption is controlled only by surface charge, has been used to characterize the adsorption of metal ions from solution on various supports. According to this model, the reaction of metal ions with ionizable surface sites is the primary mode of transfer from solution to the surface [26]. As the PZC of the support is decreased toward the pH of the impregnating solution, the amount of adsorbed anions should decrease [25]. An example of this can be found with molybdenum where the adsorption of molybdates by alumina, at constant solution pH, was studied while altering the PZC of alumina by impregnation of fluorine [28]. The

amount of adsorbed molybdates decreased as the PZC of the fluorinated alumina decreased.

This paper presents experimental verification of the effect of PZC on the hydrated structures of metal oxide overlayers. The structures of the metal oxide overlayers formed by molybdenum and tungsten oxides on alumina at the PZC of the sample are shown to correlate with the structures assumed by aqueous oxyanions at a pH equal to the PZC.

## 2. Experimental

Ketjen 000-1.5E (190 m<sup>2</sup>/g)  $\gamma$ -alumina support was used as received. The supported metal oxide samples were prepared by the conventional incipient wetness technique using aqueous solutions of (NH<sub>4</sub>)<sub>6</sub>Mo<sub>7</sub>O<sub>24</sub> (Aldrich), and (NH<sub>4</sub>)<sub>6</sub>H<sub>2</sub>W<sub>12</sub>O<sub>40</sub> (Aldrich). The samples were dried at 120°C for 3 h and calcined at 500°C for 16 h. Samples were prepared with weight loadings, which varied from 0.5 to 15 wt% Mo and from 0.5 to 30 wt% W.

The PZC of the Al<sub>2</sub>O<sub>3</sub>, Mo/Al<sub>2</sub>O<sub>3</sub>, and W/Al<sub>2</sub>O<sub>3</sub> samples was determined by the mass titration method [29]. A 0.1 M NaCl solution was prepared using distilled, deionized, and degassed water. Various amounts of solid samples were added to erlenmeyer flasks and sealed. The flasks were evacuated and backfilled with nitrogen. The NaCl solution was transferred to the flasks under a nitrogen atmosphere. Typical oxide/solution mass ratios were 0.1, 0.5, 1, 5, and 10%. The oxide/water solutions were stirred overnight with a magnetic stirrer. The pH of each solution was measured after 24 h of stirring. The pH meter was calibrated with commercial buffer solutions of pH 7 and either pH 4 or pH 10 before each measurement.

The LRS instrument and techniques have been described previously [13]. The samples were pressed into wafers and spun at 2000 rpm to avoid local heating or decomposition. The samples were calcined overnight at 500–600°C to minimize background fluorescence. The spectra were recorded after removal from the oven.

The amount of water adsorbed on the samples in an ambient environment was determined via thermal gravimetric analysis (TGA) with a Perkin-Elmer TGA 7 instrument. Twenty milligrams of sample were used. The samples were ramped from 20 to 600°C at 20°C/min.

## 3. Results

The PZC for Mo/Al<sub>2</sub>O<sub>3</sub> and W/Al<sub>2</sub>O<sub>3</sub> is presented in fig. 1 as a function of metal loading. At low supported-metal loading, the PZC of each sample was approximately that of the alumina support, 7.7. With increased Mo or W

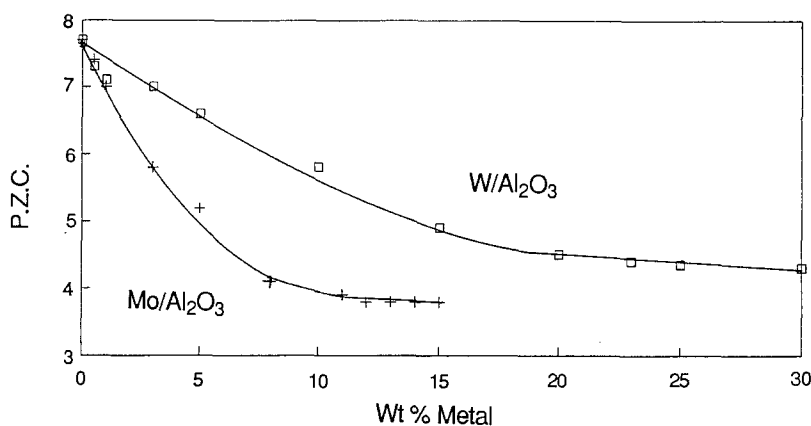


Fig. 1. Plot of point of zero surface charge versus weight loading for molybdenum (+) and tungsten (□) oxides supported on alumina.

loading, an asymptotic value of the PZC was reached, 3.7 for Mo/Al<sub>2</sub>O<sub>3</sub> and 4.3 for W/Al<sub>2</sub>O<sub>3</sub>.

The corresponding Raman spectra of the supported metal oxides are shown in figs. 2 and 3. The alumina used in this study exhibits no Raman features in the 100–1000 cm<sup>-1</sup> range. Two surface molybdate species were observed from the Raman data, an isolated, tetrahedrally-coordinated molybdate and an octahedrally-coordinated polymolybdate. No crystalline MoO<sub>3</sub> was observed on these samples. The lower molybdenum loadings, 1 and 3 wt%, exhibit bands consistent with both the tetrahedral molybdate and octahedral polymolybdate structure. The 1 wt% Mo/Al<sub>2</sub>O<sub>3</sub> sample exhibits the δ(Mo–O) bending mode at 320 cm<sup>-1</sup> of the tetrahedrally-coordinated surface molybdate and the ν(Mo–O) stretch at 924 cm<sup>-1</sup> is in the range (910–930 cm<sup>-1</sup>) normally associated with the monomeric molybdate (fig. 2a) [14]. Small amounts of the polymolybdate may be seen as evident by the Mo–O–Mo deformation mode at 219 cm<sup>-1</sup>. The tetrahedral molybdate δ(Mo–O) mode at 321 cm<sup>-1</sup> is more evident in the 3 wt% sample (fig. 2b). At 8 wt% Mo/Al<sub>2</sub>O<sub>3</sub>, the octahedrally-coordinated polymolybdate species predominated (fig. 2c). The polymolybdate bands at 356 and 219 cm<sup>-1</sup> are clearly present. The ν(Mo–O) stretch is now at 948 cm<sup>-1</sup>. The Raman bands associated with the polymolybdate species increased for the 13 wt% Mo sample (fig. 2d). An additional Raman mode was seen at 834–845 cm<sup>-1</sup>. Similar Raman bands have been reported in other Mo<sup>6+</sup>/Al<sub>2</sub>O<sub>3</sub> studies and have been attributed to a low-frequency Mo–O stretching mode [2], a high-frequency Mo–O–Mo stretching mode [2], an Al–O–Mo stretching mode [30], and to the antisymmetric Mo–O–Mo stretch for high Mo loadings [21].

Raman bands of the aqueous tetrahedral WO<sub>4</sub><sup>2-</sup> species have been assigned as a ν<sub>s</sub>(W–O) stretch at 931 cm<sup>-1</sup>, a ν<sub>as</sub>(W–O) stretch at 834 cm<sup>-1</sup>, and a δ(W–O) mode at 326 cm<sup>-1</sup> [21,22]. The aqueous octahedral W<sub>12</sub> polyanions

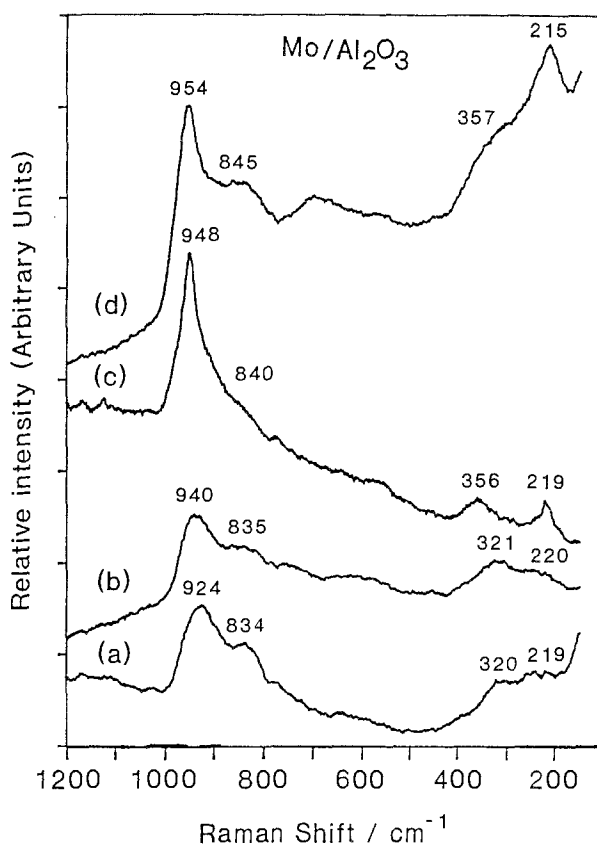


Fig. 2. Raman spectra of calcined, hydrated  $\text{Mo}^{6+}/\text{Al}_2\text{O}_3$  samples: (a) 1 wt%  $\text{Mo}/\text{Al}_2\text{O}_3$ , (b) 3 wt%  $\text{Mo}/\text{Al}_2\text{O}_3$ , (c) 8 wt%  $\text{Mo}/\text{Al}_2\text{O}_3$  and (d) 13 wt%  $\text{Mo}/\text{Al}_2\text{O}_3$ .

display a  $\nu(\text{W}-\text{O})$  stretch at  $980\text{--}960\text{ cm}^{-1}$  and a  $\text{W}-\text{O}-\text{W}$  mode at  $330\text{--}190\text{ cm}^{-1}$ . Crystalline  $\text{WO}_3$  Raman modes are located at 808, 714, and  $276\text{ cm}^{-1}$  [18].

Similar to molybdenum, two surface-supported tungstate species were observed from the Raman spectra. Additionally, crystalline  $\text{WO}_3$  was present on the 10% W sample and the 20% W sample; the crystalline  $\text{WO}_3$  Raman features are seen at 800, 695, and  $264\text{ cm}^{-1}$  (figs. 3b, 3c) [15]. Since the Raman cross-section for crystalline  $\text{WO}_3$  is 160 times larger than that for surface supported tungsta [18], it is proposed that only a small amount of the tungsten is in the crystalline form. At 2 wt% W, a surface-supported, tetrahedrally-coordinated tungstate species predominates (fig. 3a). The tetrahedral tungstate exhibits bands at 950,  $815\text{ cm}^{-1}$ , and a broad band centered at  $320\text{ cm}^{-1}$ . Small amounts of the surface-supported, octahedrally-coordinated polytungstate species may also be present at 2 wt%. Both the tetrahedral tungstate and the octahedral polytungstate are present in the 10 wt% sample as evidenced by the same tetrahedral tungstate bands as in the 2 wt% sample as well as the 230

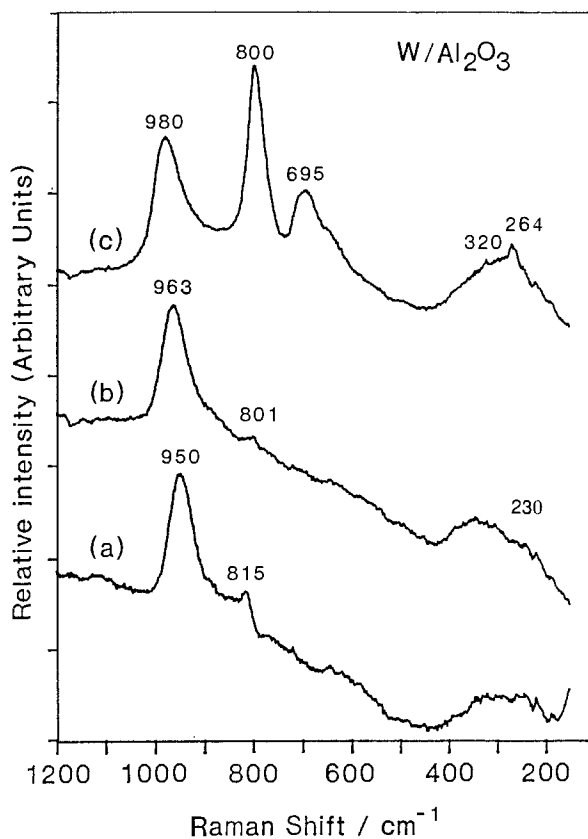


Fig. 3. Raman spectra of calcined, hydrated  $W^{6+}/Al_2O_3$  samples: (a) 2 wt%  $W/Al_2O_3$ , (b) 10 wt%  $W/Al_2O_3$  and (c) 20 wt%  $W/Al_2O_3$ .

$cm^{-1}$  band associated with the W–O–W mode of octahedrally-coordinated  $W_{12}$  polyoxoanions (fig. 3b). The 20 wt% sample exhibits increases for the  $980\text{ cm}^{-1}$  band of the polytungstate species (fig. 3c).

The amount of water adsorbed by the samples from the ambient environment was determined by TGA. Approximately 6.5% by weight of the 1 wt%  $Mo/Al_2O_3$  sample and 4.5% of the 8 wt%  $Mo/Al_2O_3$  sample was water. The water was determined to be totally desorbed by 250°C.

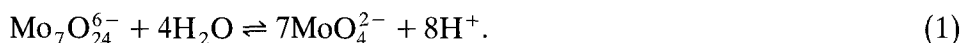
#### 4. Discussion

The PZC of all the samples decreased with increasing weight loading. The PZC decreased from the zero-coverage limit to asymptotic values because the supported metal ions modified the surface of the alumina and because the PZC of the supported molybdena and tungsta were also probed by the measurement.

The PZC decreased since molybdena and tungsta both have a PZC lower than the alumina support.

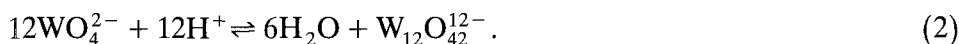
The Raman spectra were of calcined samples that were maintained in an ambient environment. Under the ambient conditions at which the Raman spectra were obtained, the oxide support was hydrated and the surface-supported molybdate or tungstate species were solvated by the water on the surface. From TGA measurements of the 1 wt% Mo/Al<sub>2</sub>O<sub>3</sub> sample and the 8 wt% Mo/Al<sub>2</sub>O<sub>3</sub> sample, the molybdenum concentration is equivalent to a 1.6 and 18.1 M solution, respectively. The surface molybdates and tungstates on alumina respond to this aqueous environment and form structures that are analogous to the structures formed in highly concentrated aqueous solutions at a pH equal to the PZC of the Mo/Al<sub>2</sub>O<sub>3</sub> or W/Al<sub>2</sub>O<sub>3</sub> sample. These structures are not dependent upon the precursor or the method of preparation [13,14].

The changes in the structure of molybdenum anions with pH and molybdenum concentration have been well characterized [21,22,31,32]. The equilibrium between the heptamolybdate species and the monomeric species is described by the expression



At Mo concentrations above 10<sup>-4</sup> M and below pH 6.8, Mo<sub>7</sub>O<sub>24</sub><sup>4-</sup>(O<sub>h</sub>) forms. Above pH 7, MoO<sub>4</sub><sup>2-</sup>(T<sub>d</sub>) predominates in solution. Both of the species are present between pH 5 and 6.8. The amount of each species, MoO<sub>4</sub><sup>2-</sup> and Mo<sub>7</sub>O<sub>24</sub><sup>6-</sup>, is dependent upon the pH and molybdenum concentration. In very acidic solutions (pH < 2.2), the octahedrally-coordinated Mo<sub>8</sub>O<sub>26</sub><sup>6-</sup> polyanion forms [22].

Above a W concentration of 0.1 M, aqueous tungstate anions exist in two structures: a tetrahedrally-coordinated WO<sub>4</sub><sup>2-</sup> anion and an octahedrally-coordinated W<sub>12</sub> polyoxoanion [21,22]. One such equilibrium between these two species is described by [32]



In alkaline solutions the tungstate monomer is the predominate species and is stable in neutral solutions. The polytungstate species is present at pH 7–8 and is the predominant species in acidic solutions. The amount of each anion species present is dependent upon the pH of the solution and the tungsten concentration.

At low supported metal oxide loading, < 3 wt% Mo or < 2 wt% W, the PZC was approximately 7. This corresponds to a neutral or even slightly alkaline aqueous solution and tetrahedrally-coordinated molybdate and tungstate structures are expected to form. The Raman data (figs. 2a and 3a) demonstrate the formation of tetrahedrally-coordinated Mo and W structures. Similarly, the surface-supported, octahedrally-coordinated polymolybdate and polytungstate structures (figs. 2d and 3c) found at the asymptotic PZC, 3.7 for Mo and 4.3 for

W, are analogous to the polyanions found in aqueous solutions at a pH equal to the PZC. The PZC of both the Mo/Al<sub>2</sub>O<sub>3</sub> and W/Al<sub>2</sub>O<sub>3</sub> samples decreased rapidly from the zero-coverage value at low metal loadings. In aqueous molybdate solutions, both the tetrahedrally-coordinated MoO<sub>4</sub><sup>2-</sup> and the octahedrally-coordinated Mo<sub>7</sub>O<sub>24</sub><sup>6-</sup> anions are present in this pH region. In aqueous tungstate solutions, both the tetrahedrally-coordinated WO<sub>4</sub><sup>2-</sup> and octahedrally-coordinated W<sub>12</sub> polyoxoanions are present in this pH region. From the Raman data (figs. 2b and 3b), it is observed that both the tetrahedral molybdate and octahedral polymolybdate structures are present on the Mo/Al<sub>2</sub>O<sub>3</sub> samples and both the tetrahedral tungstate and the octahedral polytungstate structures are present on the W/Al<sub>2</sub>O<sub>3</sub> samples.

Additional evidence for a relationship between PZC and oxide structure can be found with Mo/SiO<sub>2</sub>. The PZC of silica samples used in other studies [13] has been found to be 3.7. Adding molybdenum to the surface of the silica decreased the PZC. The PZC of 0.1 and 0.5 wt% Mo/SiO<sub>2</sub> was found to be 3.4 and 2.9, respectively [33]. Therefore, the surface of hydrated silica is equivalent to a low-pH solution. Octahedrally-coordinated molybdenum clusters have been found to form on silica at all Mo loadings [13]. Since the PZC of Mo/SiO<sub>2</sub> cannot exceed the PZC of SiO<sub>2</sub>, only octahedrally-coordinated polymolybdates should be found, which is in agreement with recent Raman [13,14] and XANES/EXAFS [34] results.

The results presented here show that the PZC controls the structure of supported metal oxide overlayers. The hydrated structures form upon exposure of the calcined oxides to an ambient environment. The structures of molybdate and tungstate overlayers on alumina are similar to the structure formed by aqueous molybdate and tungstate anions at a pH equal to the PZC.

## Acknowledgement

This work was supported by the US Department of Energy, Office of Basic Energy Sciences (SDK and JGE). The authors acknowledge Mom-Ping Ng for help in performing the PZC measurements.

## References

- [1] J. Medema, C. van Stam, V.H.J. de Beer, A.J.A. Konings and D.C. Koningsberger, *J. Catal.* 53 (1978) 386.
- [2] H. Jeziorowski and H. Knözinger, *J. Phys Chem.* 83 (1979) 1166.
- [3] C.P. Cheng and G.L. Schrader, *J. Catal.* 60 (1979) 276.
- [4] D.S. Zingg, L.E. Makovsky, R.E. Tischer, F.R. Brown and D.M. Hercules, *J. Phys. Chem.* 84 (1980) 2898.
- [5] P. Dufresne, E. Payen, J. Grimblot and J.P. Bonnelle, *J. Phys. Chem.* 85 (1981) 2344.



- [6] J.M. Stencel, L.E. Makovsky, T.A. Sarkus, J. de Vries, R. Thomas, and J.A. Moulijn, *J. Catal.* 90 (1984) 314.
- [7] E. Payen, S. Kasztelan, J. Grimblot and J.P. Bonnelle, *J. Raman Spectry.* 17 (1986) 233.
- [8] J.A.R. van Veen and P.A.J.M. Hendriks, *Polyhedron* 5 (1986) 75.
- [9] J.A.R. van Veen, H. de Wit, C.A. Emeis and P.A.J.M. Hendriks, *J. Catal.* 107 (1987) 579.
- [10] E. Payen, J. Grimblot and S. Kasztelan, *J. Phys. Chem.* 91 (1987) 6642.
- [11] Y. Okamoto and T. Imanaka, *J. Phys. Chem.* 92 (1988) 7102.
- [12] J.A.R. van Veen, P.A.J.M. Hendriks, E.J.G.M. Romers and R.R. Andrea, *J. Phys. Chem.* 94 (1990) 5275.
- [13] C.C. Williams, J.G. Ekerdt, J. Jehng, F.D. Hardcastle, A.M. Turek, and I.E. Wachs, *J. Phys. Chem.* 95 (1991) 8781.
- [14] C.C. Williams, J.G. Ekerdt, J. Jehng, F.D. Hardcastle and I.E. Wachs, *J. Phys. Chem.* 95 (1991) 8781.
- [15] J.M. Stencel, L.E. Makovsky, J.R. Diehl and T.A. Sarkus, *J. Raman Spectry.* 15 (1984) 283.
- [16] S.S. Chan, I.E. Wachs, L.L. Murrell, I. Wang and W.K. Hall, *J. Phys. Chem.* 88 (1984) 5831.
- [17] J.A. Horsley, I.E. Wachs, J.M. Brown, G.H. Via and F.D. Hardcastle, *J. Phys. Chem.* 91 (1987) 4014.
- [18] S.S. Chan, I.E. Wachs and L.L. Murrell, *J. Catal.* 90 (1984) 150.
- [19] S.S. Chan, I.E. Wachs, L.L. Murrell and N.C. Dispenziere Jr, *J. Catal.* 92 (1985) 1.
- [20] I.E. Wachs and G. Deo, *J. Phys. Chem.* 95 (1991) 5889.
- [21] W.P. Griffith and P.J.B.J. Lesniak, *J. Chem. Soc. A* (1969) 1066.
- [22] C.F. Baes and R.E. Mesmer, in: *The Hydrolysis of Cations* (Wiley, New York, 1986).
- [23] W.J. Stumm and C.P. Huang, *J. Colloid Interface Sci.* 43 (1973) 409.
- [24] W.J. Stumm and H. Hohl, *J. Colloid Interface Sci.* 55 (1976) 281.
- [25] J.P. Brunelle, *Pure Appl. Chem.* 50 (1978) 1211.
- [26] J.A. Davis, R.O. James and J.O. Leckie, *J. Colloid Interface Sci.* 63 (1978) 480.
- [27] L. Wang and W.K. Hall, *J. Catal.* 77 (1982) 232.
- [28] F.M. Mulcahy, M. Houalla and D.M. Hercules, *J. Catal.* 106 (1987) 210.
- [29] J.S. Noh and J.A. Schwartz, *J. Colloid Interface Sci.* 130 (1989) 157.
- [30] S. Kasztelan, E. Payen, H. Toulhoat, J. Grimblot and J.P. Bonelle, *Polyhedron* 5 (1986) 157.
- [31] N.P. Luthra and W.C. Cheng, *J. Catal.* 107 (1987) 154.
- [32] J. Aveston, E.W. Anacker and J.S. Johnson, *Inorg. Chem.* 3 (1969) 735.
- [33] S.D. Kohler, unpublished.
- [34] M. de Boer, A.J. van Dillen, D.C. Koningsberger, J.W. Geus, M.A. Vuurman and I.E. Wachs, *Catal. Lett.* 11 (1991) 227.